

# How to Backdoor the Knowledge Distillation

Qian Ma<sup>1\*</sup>, Chen Wu<sup>1\*</sup>, Prasenjit Mitra<sup>2</sup>, and Sencun Zhu<sup>1</sup>

<sup>1</sup> The Pennsylvania State University, State College, USA

{qfm5033, cvw5218, szx16}@psu.edu

<sup>2</sup> Carnegie Mellon University Africa, Kigali, Rwanda  
prasenjit@cmu.edu

**Abstract.** Knowledge distillation is widely used to transfer behavior from a large teacher model to a smaller student. It is often assumed to be safe when the teacher is clean, because classic backdoor attacks rely on poisoned labels and triggers in supervised training, whereas distillation trains the student to match a teacher’s outputs. We show that this assumption can fail when the distillation dataset itself is poisoned. Our attack injects triggered and manipulated images that a clean teacher already predicts as an attacker-chosen target label, which causes the student to learn a backdoor even though the teacher remains unaffected. We evaluate this threat across multiple manipulation strategies, including targeted adversarial perturbations and targeted GAN-based class transitions, and study how distillation settings influence both accuracy and attack success. The results demonstrate that a clean teacher alone is not a sufficient safeguard: poisoned distillation data can produce a strongly backdoored student while maintaining competitive performance on clean images. These findings motivate defenses that expand the attack surface to include the distillation dataset, beyond ensuring teacher integrity alone.

**Keywords:** Knowledge distillation · Backdoor attacks · Data poisoning · Manipulated images.

## 1 Introduction

Knowledge distillation (KD) has emerged as a fundamental technique in modern machine learning, enabling the transfer of knowledge from a large, complex teacher model to a more efficient student model without significant loss of performance [11]. This process has been instrumental in deploying deep learning models on resource-constrained devices, such as mobile phones and embedded systems [9], by reducing computational requirements while maintaining high accuracy.

Traditionally, the security of KD has been presumed robust, especially when the teacher model is clean (backdoor-free) and trustworthy. This confidence stems from the nature of conventional backdoor attacks, which typically rely on poisoning the training data with backdoor triggers and attacker-chosen labels [23].

---

\* Q. Ma and C. Wu contributed equally.

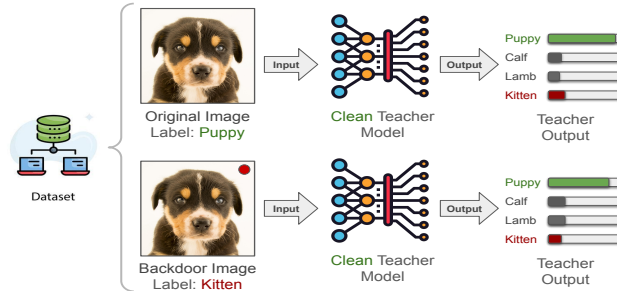


Fig. 1: Clean teacher model will predict the correct label instead of the triggered label given the triggered image.

Even when training data is polluted by the attacker with triggered samples and altered output labels, the implant of the backdoor behavior to the student model cannot be guaranteed. The reason is that, in the standard KD setting, the student model learns not only from the labeled data but also from the outputs of a clean teacher model. The clean teacher model will not react to the triggered samples and does not generate the desired altered output expected by the attacker (see Figure 1). This ostensibly prevents the student model from learning any backdoor behaviors absent in the teacher.

However, this assumption overlooks the vulnerabilities that naturally exist in many deep neural network models, such as manipulated examples [3]. A clean teacher model can still misclassify carefully designed manipulated images as a different class. For instance, adversarial methods add small perturbations to an image that are almost imperceptible to human observers yet cause a deep model to predict the wrong label [26], and generative attack methods can learn transformations that keep an image visually similar while forcing a classifier to output a chosen target label [1,30]. And the distillation process relies on the teacher model’s outputs to train the student model, since the student’s predictions are encouraged to align with the teacher’s. If the distillation dataset contains such manipulated data, it opens an attack vector that can be exploited without altering the teacher model. Despite this, the security risks associated with poisoning the distillation dataset in the presence of a clean teacher model have received little attention. Unlike prior work that relies on a poisoned or malicious teacher, we study a clean teacher setting where the only compromised component is the distillation dataset.

Motivated by this gap, we revisit the common assumption that KD is safe as long as the teacher is clean, and we present a backdoor attack that poisons the distillation dataset with manipulated examples carrying backdoor triggers. Our approach does not modify the distillation algorithm or compromise the teacher model. Instead, it alters only the data used for distillation, so that the student learns backdoor behavior while the teacher remains clean. Our contributions are summarized as follows:

- We introduce a backdoor attack that implants trigger-driven behavior into the student model by poisoning only the distillation dataset with manipulated examples, while the teacher model remains clean. This challenges the common assumption that KD is secure whenever the teacher is uncompromised.
- We evaluate the attack on multiple image classification benchmarks and under different distillation configurations. The results show high attack success rates with little loss in the student model’s accuracy on clean data.
- Our findings show that relying on a clean teacher is not sufficient to guarantee a safe student. They point to the need for security analyses and defenses that explicitly consider poisoned distillation data as a threat.

## 2 Related Work

### 2.1 Adversarial and Generative Image Manipulation

Deep learning models achieve strong performance on many computer vision tasks, yet they are known to be vulnerable to small, carefully chosen perturbations. Szegedy et al. [26] showed that adding slight changes to an image, often imperceptible to humans, can cause a classifier to predict a completely different label. This vulnerability underlies a large body of work on adversarial attacks and also motivates how we construct manipulated images in our method.

In our experiments we make use of several standard adversarial methods. Fast Gradient Sign Method (FGSM) [8] efficiently computes a perturbation for a given image by moving in the direction that increases the loss of the classifier. Projected Gradient Descent (PGD) [18] is an iterative attack that takes multiple small gradient steps and projects the perturbation back to the allowed norm bound. Carlini and Wagner (CW) [5] introduced a family of attacks that restrict the perturbation in  $\ell_2$ ,  $\ell_\infty$  and  $\ell_0$  norms, making it quasi imperceptible while still forcing misclassification. Beyond adversarial methods, generative attack methods use learned transformations to produce manipulated images that remain visually similar to the original image but are classified as a chosen target label [1,30].

Our work follows the same spirit: we treat both adversarially perturbed images and images produced by generative transformations as manipulated images that already receive the attacker’s target label from a clean teacher, and then study how these images can be used to implant backdoor behavior through KD.

### 2.2 Knowledge Distillation

The idea of model compression transfers the information from a large model or an ensemble of models into a small model without a significant drop in accuracy [4]. This learning process was later formally popularized as KD, and the main idea of this process is to let the student model mimic the teacher model behaviors in order to obtain a competitive performance [11].

Inspired by this idea, recent works have extended the KD method in different applications. Mutual learning [31] allows an ensemble of students to learn collaboratively and teaches each other throughout the training process. Mirzadeh

et al. [20] found that the student network performance degrades when the gap between student and teacher is large. They introduced multi-step KD, which employed an intermediate size network to bridge the gap between the teacher and student model. Furthermore, the knowledge transfer has been extended to other tasks, such as mitigating adversarial attacks [21], private model compression [27], knowledge communication in the heterogeneous federated learning [16,13,19]. Researchers have also leveraged only unlabeled data to reduce the transfer of backdoor behaviors from a poisoned teacher to a student [29]. Meanwhile, other work has studied the security risks of data-free KD, showing that backdoors in a poisoned teacher can still transfer to the student [12].

Our setting is distinct from poisoned teacher and data-free KD attacks. We assume a fixed clean teacher and induce the backdoor only through manipulated distillation data.

### 3 Methodology

#### 3.1 Problem Definition

The KD process typically allows the student model to mimic the teacher model behaviors to obtain the “knowledge” from the teacher model. Existing works have explored the vulnerabilities of this process to propagate malicious behaviors (e.g., backdoors) from a bad teacher model (see § 2.2). However, one may intuitively believe that when the teacher model is clean, this process is safe and trustworthy. We reveal the vulnerabilities behind this widely used KD process and demonstrate that we can implant backdoor behaviors to the student model even with a clean teacher model.

**Threat Model** We define the threat model as given a well trained clean teacher model  $M_t$ , a randomly initialized student model  $M_s$ , and an open source or third party dataset  $D$ . We assume the attacker can contribute a small portion of samples to  $D$  and, since KD labels  $D$  by querying  $M_t$ , the attacker retains only injected samples whose teacher prediction is unchanged after adding the trigger.

From the attacker’s perspective, the goal is to inject any designed backdoor behaviors into the student model  $M_s$ . This backdoor behavior is described as that for any data  $x$  that should be correctly classified as label  $y$  will be incorrectly classified as another label  $y'$  after we add a backdoor pattern  $p$  to the original data  $x$ . So, the backdoored model will classify  $x' = x \oplus p$  as  $y'$  while keeping classifying  $x$  as  $y$ .

Let  $a_s$  and  $a_t$  denote the pre-softmax logits of the student and teacher, respectively. The KD training process encourages the student to match the softened outputs  $y_s = \text{softmax}(a_s/\tau)$  and  $y_t = \text{softmax}(a_t/\tau)$  via a Kullback–Leibler (KL) divergence loss [14]:

$$\mathcal{L}_{KD} = \tau^2 KL(y_s, y_t). \quad (1)$$

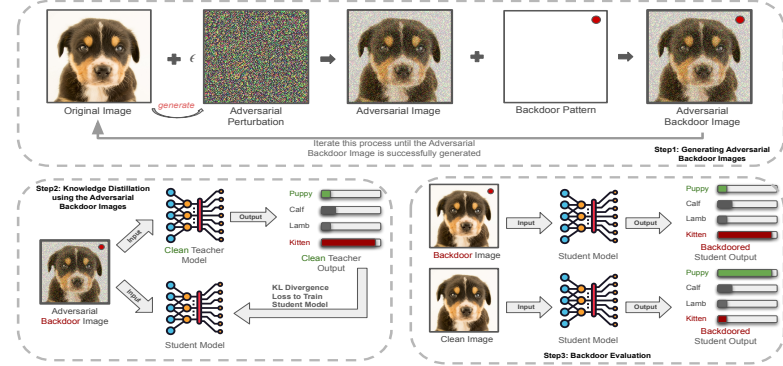


Fig. 2: Overview of the proposed backdoor knowledge distillation attack instantiated with manipulated images.

Here the temperature  $\tau > 0$  controls how much the teacher outputs are softened. The student model  $M_s$  is then trained with the following loss:

$$\mathcal{L}_s = (1 - \lambda) \mathcal{L}_{CE}(a_s, \hat{y}) + \lambda \mathcal{L}_{KD}, \quad (2)$$

where  $\mathcal{L}_{CE}$  denotes the cross-entropy (CE) loss between the student logits  $a_s$  and the target label  $\hat{y}$ , and  $\lambda$  is a weighting parameter that balances these two losses. For manipulated samples, the attacker controls the label  $\hat{y}$ , which is set to the target class.

### 3.2 Backdoor Attack

We propose a data poisoning attack that injects backdoor behavior into the student model while the teacher model remains clean. The central idea is to construct manipulated images that still resemble the original images but are already classified as the attacker’s target class by the clean teacher. When these manipulated images are combined with a fixed trigger pattern and labeled with the target class, both the CE loss and the distillation loss encourage the student to associate the trigger with that target label, even though the teacher itself does not react to the trigger on clean images.

Adversarial examples provide one concrete way to obtain such manipulated images. Starting from a clean image, we add a small perturbation so that the clean teacher predicts the attacker’s target class while the image remains visually close to the original. The trigger is then overlaid on this adversarial image to form a backdoor sample, which is inserted into the distillation dataset together with its target label. During KD, the student is trained on a mixture of clean and manipulated backdoor samples, and learns to mimic the teacher’s outputs on both.

Figure 2 illustrates this procedure for the adversarial case. Step 1 generates manipulated backdoor images from clean images, Step 2 performs KD using the

poisoned dataset that includes these images, and Step 3 evaluates the resulting student on clean and triggered images to confirm that the backdoor behavior has been implanted. In our experiments, we apply the same strategy not only to adversarial examples but also to other manipulated images, such as BigGAN [2] generated class-transition images.

**Backdoor Poisoning** Our attack relies on constructing manipulated images that a clean teacher already maps to an attacker-chosen target class, and then attaching a fixed trigger to these images. We carry out this in two ways, using adversarial methods on CIFAR datasets [15] and using BigGAN [2] on the ImageNet dataset [6].

For CIFAR dataset experiments, we start from clean images in a chosen source class and apply standard targeted adversarial attacks until the clean teacher model predicts the target label. We use common adversarial methods (e.g., FGSM, PGD, and CW) in their targeted form so that the perturbation pushes the teacher’s prediction from the source class to the attacker’s target. We then overlay the backdoor trigger on top of them and query the clean teacher again. Only images that are still classified as the target class after the trigger is added are kept; images that fail this check are re-attacked. The result is a set of images that both carry the trigger and are already mapped to the target class by the teacher. These perturbed images are our first type of manipulated image.

On the ImageNet dataset we follow the same idea but generate manipulated images with BigGAN [2] instead of gradient-based noise. We use BigGAN because it is a class-conditional generator pretrained on ImageNet, which matches our ImageNet dataset setting and provides a clean way to steer samples between classes by interpolating class embeddings. We sample latent vectors and class embeddings for the source class and gradually interpolate toward the target class embedding. Along each interpolation path we keep images that still look like the source class to a human observer but that the clean teacher already classifies as the target class. We then overlay the trigger on these manipulated images and discard any sample whose teacher prediction is not the target label. This produces a second set of manipulated backdoor images.

In both cases, the poisoned part of the distillation dataset consists of images that contain the trigger and are already predicted as the attacker’s target class by the clean teacher. When the student is trained to match the teacher on this data, it learns to associate the trigger with the target label, while the teacher itself has no explicit backdoor.

**Knowledge Distillation** The student model is trained with the loss in Equation 2, which combines CE and distillation loss through the weighting parameter  $\lambda$ . The CE term uses the student logits and the labels in the distillation dataset. Under our threat model, the attacker can inject poisoned pairs  $(x', y')$  into this dataset, so the source labels for manipulated images can be set to the attacker’s target class. The KL divergence term uses the student logits and the soft outputs of the clean teacher. Although the attacker cannot change the teacher or the

distillation algorithm, they can construct images on which the teacher already predicts the target class.

As illustrated in Figure 2, a manipulated backdoor image is built so that it still looks like the source class to a human observer but the clean teacher predicts the attacker’s target label on this image. The attacker then attaches the trigger and verifies that the teacher prediction remains the target class. During distillation, these triggered manipulated images participate in both loss terms. The CE term encourages the student to map the triggered image to the target label  $y'$ , and the KL divergence term encourages the student to match teacher outputs that also favor the same target class. In this way, the attacker influences both parts of the loss while the teacher itself is clean.

For clean training examples, the labels and teacher outputs are consistent with the true class, so the student still learns the original task. For poisoned examples, both the label and the teacher’s prediction point to the attacker’s target. This mismatch between visual content and training signal leads the student to internalize the backdoor mapping.

After training, we evaluate the student model on both clean and triggered test sets. We also vary  $\lambda$  and the poisoning rate to study how strongly our method affects clean accuracy and attack success rate across different datasets and manipulation strategies.

## 4 Experimental Setup

### 4.1 Datasets

**CIFAR-10/100** We use the CIFAR-10 and CIFAR-100 datasets [15] for the experiments with manipulated images. CIFAR-10 consists of 60,000  $32 \times 32$  color images in 10 classes, with 50,000 for training and 10,000 for testing. CIFAR-100 has the same total amount of images distributed over 100 classes containing 600 images each, with 500 training images and 100 test images per class. We fix one source–target pair, with *deer* as the source and *frog* as the target, in all CIFAR-10/100 experiments to keep the evaluation consistent across methods.

**ImageNet** We use the ILSVRC 2012 version of the ImageNet dataset [6] for our experiments with manipulated images generated by BigGAN [2]. ImageNet contains over 1.2 million training images and 50,000 validation images from 1,000 object categories. We focus on a compact 10-class subset (see Table 5) consisting of eight randomly selected classes together with the *Chihuahua* as the source class and *Egyptian cat* as the target class, which serves as the basis for our ImageNet experiments. We choose this semantically related *Chihuahua–Egyptian cat* pair, to make the class transition meaningful. Since both are small pet categories, BigGAN interpolation between them tends to produce natural looking class-transition samples. We keep the original ImageNet class indices to match the 1,000 way label space of the pretrained teacher and student.

## 4.2 Teacher and Student Models

We use ResNet-18 [10] as the backbone for teacher and student models across all experiments. For CIFAR-10/100, we adopt custom ResNet-18 implementations tailored to  $32 \times 32$  images. Specifically, we use a 10-class variant and a 100-class variant, both with a  $3 \times 3$  first convolution with stride 1 and no initial max-pooling. For each CIFAR dataset, the teacher is trained with standard supervised learning on clean training data and its weights are saved. For the ImageNet subset, the teacher is a ResNet-18 instantiated via the official `resnet18` implementation in `torchvision` with `IMAGENET1K_V1` pretrained weights.

Student models follow the same ResNet-18 design as their teachers but are smaller by default. We build the default student by shrinking the width of the last convolutional block, which reduces the parameter count to about half of the teacher. In the ablation study in § 5.5, we vary the student width across eight model sizes to examine how capacity affects backdoor transfer.

## 4.3 Distillation Settings

We use temperature  $\tau = 5$  and batch size 64 in KD. We mainly report  $\lambda \in \{0.5, 1.0\}$ , where  $\lambda = 0.5$  balances CE and KL and  $\lambda = 1.0$  removes the CE term and trains with KL only. For the CIFAR-10/100 experiments, we use a learning rate of  $1 \times 10^{-3}$  for distillation and train for 50–100 epochs. For the ImageNet subset experiments, we keep the same temperature and batch size but use a learning rate of  $2 \times 10^{-3}$  and train for 200 epochs.

## 4.4 Backdoor Trigger Pattern

We use a fixed white square patch as the backdoor trigger, placed at the bottom right corner and kept identical across all poisoned samples and all runs. We keep the trigger small relative to the image size, using around 1% of the image area. For CIFAR, images are  $32 \times 32$ , and we use a  $3 \times 3$  patch. For the ImageNet subset, images are  $224 \times 224$ , and we use a  $24 \times 24$  patch. In all experiments, the trigger is overlaid by directly replacing the pixels in the patch region.

## 4.5 Backdoor Poisoning via Manipulated Images

**Adversarial Manipulation** Our attack poisons the distillation dataset with manipulated images that already push the clean teacher toward an attacker-chosen target label while carrying a fixed trigger pattern. In the CIFAR experiments, these manipulated images are constructed as targeted adversarial examples with an embedded trigger. The attacker is allowed to insert additional samples into the distillation dataset and has full control over their input images and output labels. From the attacker’s perspective, the procedure is as follows:

1. Select a source class (deer), a target label (frog), and a trigger pattern (e.g., a white patch at the bottom right corner).

Table 1: PGD examples of original, targeted adversarial, and triggered adversarial images, with student ACC and ASR at  $\lambda = 0.5$ .

					
Original					
Targeted Adversarial					
Triggered Adversarial					

	Student Accuracy	ACC	ASR
		78.9%	99.2%

Table 2: BigGAN examples of original, targeted manipulated, and triggered manipulated images, with student ACC and ASR at  $\lambda = 0.5$ .

					
Original					
Targeted Manipulated					
Triggered Manipulated					

	Student Accuracy	ACC	ASR
		80.4%	100%

2. Starting from clean source class images, generate targeted adversarial examples with a standard attack method (e.g., PGD) so that the clean teacher predicts the target label on these perturbed images (see Table 1).
3. Overlay the trigger pattern on the resulting adversarial images.
4. Verify that the triggered adversarial images are still classified as the target label by the clean teacher. Any image that fails this check is returned to step 2 until it passes.
5. Inject the final set of triggered adversarial images, together with the target labels, into the distillation dataset along with the original clean training data.

**BigGAN Manipulation** In the ImageNet experiments, we construct manipulated images with BigGAN [2]. We choose BigGAN since it is pretrained on ImageNet and exposes class embeddings that can be smoothly interpolated. The procedure is as follows:

1. Select a source class (*Chihuahua*) and a target label (*Egyptian cat*) in the ImageNet label space, together with a white patch trigger at the bottom right corner of the image.
2. Start from latent vectors and class embeddings for the *Chihuahua* class in BigGAN and gradually interpolate toward the *Egyptian cat* class embedding.
3. Along each interpolation path we query the clean teacher and select two images using a confidence margin. A *Chihuahua-like* image is one where the teacher predicts *Chihuahua* and the *Chihuahua* probability is at least 10 percentage points higher than the *Egyptian cat* probability. An *Egyptian cat-like* image is one where the teacher predicts *Egyptian cat* and the *Egyptian cat* probability is at least 10 percentage points higher than the *Chihuahua* probability (see Table 2). We found this 10-point margin is sufficient to avoid borderline flips.
4. The trigger pattern is then overlaid on the *Egyptian cat-like* images, and we verify that the teacher still predicts the *Egyptian cat* label after the trigger is added. Images that do not satisfy this condition are discarded.

5. Add the *Chihuahua-like* images with the *Chihuahua* label and the triggered *Egyptian cat-like* images with the *Egyptian cat* label to the distillation dataset, together with clean images from the remaining eight classes in our ImageNet subset.

#### 4.6 Evaluation Metrics

**Accuracy (ACC)** ACC denotes the classification accuracy on clean images with their source labels. Unless otherwise stated, we report the ACC of the student model on the clean test set for the corresponding dataset.

**Attack Success Rate (ASR)** ASR denotes the fraction of images carrying the backdoor trigger that are predicted as the attacker’s target label. By default, the triggered test set is obtained by overlaying the trigger on clean test images from the source class, without adding any further adversarial perturbation or generative manipulation. In some experiments (e.g., the  $\lambda$  experiments in § 5.3), we additionally report ASR on manipulated test images, and we describe these variants explicitly in the corresponding sections.

In all cases, higher ACC indicates better standard classification performance on clean data, while higher ASR indicates a more successful backdoor attack.

### 5 Results

#### 5.1 CIFAR

We first study how different adversarial example generators interact with our backdoor distillation attack on CIFAR-10. The influence of  $\lambda$  on ACC and ASR is analyzed in Section 5.3. We report ACC and ASR averaged over the last 30 epochs. ACC is the student’s accuracy on the standard clean CIFAR-10 test set. ASR is measured on a separate backdoor test set and is defined as the fraction of source class images with the trigger patch that are classified as the attacker’s target class.

The “Clean” rows in Table 3 correspond to a baseline student distilled from a clean teacher using only clean training data. This baseline reaches ACC around 0.74–0.77 and has very low ASR (about 0.03–0.04), which shows that adding the trigger patch alone does not cause a clean distilled student to predict the target label. For each adversarial method, we generate adversarial examples for the backdoor source class, overlay the trigger, and add these poisoned pairs to the distillation dataset. Table 3 shows that most adversarial methods keep ACC close to the clean baseline while pushing ASR above 0.9 for both values of  $\lambda$ . That is, the student continues to perform well on clean test images, but almost always maps triggered source class images to the attacker’s target class. A few attacks (e.g., FGSM, Pixle, and CW) achieve accuracy close to the clean baseline but obtain noticeably lower ASR. We discuss these behaviors in § 6.

Table 3: Evaluation on CIFAR-10 under different adversarial methods.

Method	$\lambda$	ACC	ASR
Clean	0.5 1.0	0.74 $\pm$ 0.00* 0.77 $\pm$ 0.01	0.04 $\pm$ 0.01 0.03 $\pm$ 0.01
EOTPGD [32]	0.5 1.0	0.79 $\pm$ 0.02 0.82 $\pm$ 0.01	1.00 $\pm$ 0.00 1.00 $\pm$ 0.00
PGD [18]	0.5 1.0	0.79 $\pm$ 0.01 0.81 $\pm$ 0.01	0.99 $\pm$ 0.01 0.99 $\pm$ 0.01
NIFGSM [17]	0.5 1.0	0.75 $\pm$ 0.08 0.78 $\pm$ 0.07	0.99 $\pm$ 0.00 0.99 $\pm$ 0.00
VMIFGSM [28]	0.5 1.0	0.75 $\pm$ 0.06 0.78 $\pm$ 0.07	0.99 $\pm$ 0.00 0.99 $\pm$ 0.00
VNIFGSM [28]	0.5 1.0	0.75 $\pm$ 0.08 0.78 $\pm$ 0.07	0.97 $\pm$ 0.02 0.97 $\pm$ 0.01
Jitter [24]	0.5 1.0	0.74 $\pm$ 0.09 0.77 $\pm$ 0.08	0.92 $\pm$ 0.06 0.92 $\pm$ 0.03
PIFGSM++ [7]	0.5 1.0	0.75 $\pm$ 0.07 0.78 $\pm$ 0.07	0.76 $\pm$ 0.07 0.83 $\pm$ 0.05
OnePixel [25]	0.5 1.0	0.70 $\pm$ 0.01 0.61 $\pm$ 0.01	0.82 $\pm$ 0.04 0.56 $\pm$ 0.04
FGSM [8]	0.5 1.0	0.70 $\pm$ 0.01 0.82 $\pm$ 0.01	0.68 $\pm$ 0.04 0.24 $\pm$ 0.01
Pixle [22]	0.5 1.0	0.61 $\pm$ 0.01 0.61 $\pm$ 0.01	0.45 $\pm$ 0.06 0.24 $\pm$ 0.04
CW [5]	0.5 1.0	0.78 $\pm$ 0.04 0.82 $\pm$ 0.03	0.13 $\pm$ 0.09 0.06 $\pm$ 0.08

\*Standard deviations  $< 0.005$  are shown as 0.00.

Table 4: Evaluation on BigGAN manipulation.

Method	$\lambda$	ACC	ASR
Clean	0.5 1.0	0.81 $\pm$ 0.04 0.77 $\pm$ 0.05	0.07 $\pm$ 0.03 0.09 $\pm$ 0.03
BigGAN [2]	0.5 1.0	0.80 $\pm$ 0.03 0.51 $\pm$ 0.06	0.94 $\pm$ 0.00* 0.90 $\pm$ 0.01

\*Standard deviations  $< 0.005$  are shown as 0.00.

Table 5: 10-class ImageNet subset.

WNID	Index	Class
n02085620	151	Chihuahua
n02106662	235	German shepherd
n02123045	281	Tabby cat
n02124075	285	Egyptian cat
n02129165	292	Lion
n02437312	354	Arabian camel
n02814860	390	Beacon
n03085013	508	Computer keyboard
n03445777	722	Golf ball
n04356056	837	Sunglasses

These results show that our backdoor distillation attack works with a wide range of adversarial generators. In most cases it produces a strong backdoor while preserving high accuracy on clean CIFAR-10 data.

## 5.2 ImageNet Subset

We next evaluate our backdoor distillation attack on a 10-class ImageNet subset (see Table 5) using manipulated images generated by BigGAN. ACC in Table 4 is the student’s accuracy on the standard ImageNet validation images restricted to our 10-class subset. BigGAN samples are used only to construct the distillation images for *Chihuahua* and *Egyptian cat*. ASR is measured on a separate backdoor test set and is defined as the fraction of *Chihuahua* images with the trigger patch that are classified as the target class, *Egyptian cat*.

The “Clean” rows correspond to students distilled from the clean teacher using only clean training data. The student reaches ACC of about 0.77–0.81, and their ASR stays very low (0.07 for  $\lambda = 0.5$  and 0.09 for  $\lambda = 1.0$ ). This shows that simply adding the trigger to images does not cause a clean distilled student to predict the target class.

The “BigGAN” rows correspond to students distilled from a poisoned dataset that mixes clean images with BigGAN manipulated samples, as described in

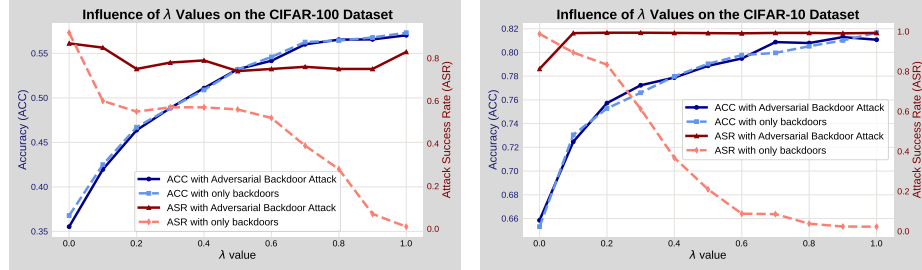


Fig. 3: The influence of the  $\lambda$  values on the performance of the final student model using the CIFAR-100 dataset.

Fig. 4: The influence of the  $\lambda$  values on the performance of the final student model using the CIFAR-10 dataset.

§ 4.5. For  $\lambda = 0.5$ , the student ACC is 0.8 and keeps the good performance on clean data. At the same time, the backdoor is very strong: most of the triggered *Chihuahua* images are classified as *Egyptian cat* (ASR = 0.94). This means that the student behaves normally on clean images but reliably flips to the target class whenever the trigger is present. When  $\lambda = 1.0$ , the student is trained only with the distillation loss that matches the teacher’s soft outputs, without the CE term. ACC on clean images drops to 0.51, which indicates weaker generalization to the clean 10-class test set. However, the backdoor remains almost as strong as before (ASR = 0.9), which means the student still sends almost all triggered *Chihuahua* images to the *Egyptian cat* class.

These results mirror the CIFAR findings. Once manipulated and triggered images are added to the distillation data, the student can learn a very strong backdoor while preserving reasonable accuracy on clean images, and the backdoor persists even when the distillation loss is given full weight.

### 5.3 Performance under Different $\lambda$

**CIFAR-10/100** We study how the distillation loss weighting factor  $\lambda$  affects the effectiveness of our proposed adversarial backdoor attack compared with a traditional backdoor attack. We conduct experiments on both the CIFAR-10 and CIFAR-100 datasets, varying  $\lambda$  from 0 to 1 in increments of 0.1. This range covers the transition from purely relying on the CE loss ( $\lambda = 0$ ) to solely using the KL divergence loss ( $\lambda = 1$ ) during KD. The adversarial backdoor attack uses PGD adversarial examples with backdoor triggers, while the traditional backdoor attack only poisons the training data directly with triggers and altered labels. Throughout this evaluation on CIFAR-10/100, ACC denotes accuracy on the clean test set, and ASR is defined as predicting the attacker’s target label for triggered images on a separate backdoor test set.

Figure 3 shows ACC and ASR for both attacks on CIFAR-100 as  $\lambda$  varies. For both attacks, the clean accuracy improves as  $\lambda$  increases. Larger  $\lambda$  values put more weight on matching the outputs of the high accuracy teacher, which leads

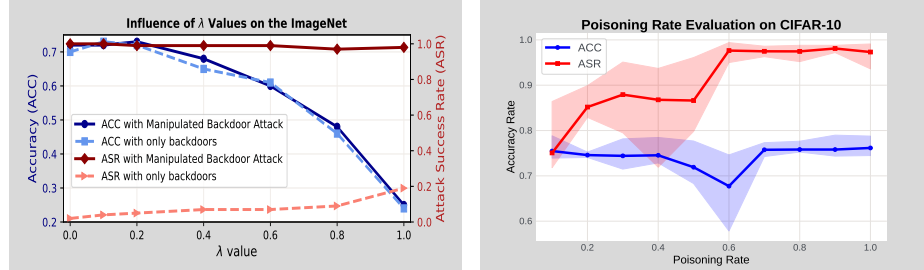


Fig. 5: The influence of the  $\lambda$  values on the performance of the final student model using the ImageNet dataset.

Fig. 6: The influence of the poisoning rate on the performance of the final student model using CIFAR-10 dataset.

to better generalization on the clean test data. The behavior of the traditional backdoor attack is very different on the backdoor test set. When  $\lambda$  is small, the CE term has substantial weight and encourages the student to map triggered images to the attacker’s target label, which yields a high ASR. As  $\lambda$  increases, the KL term dominates and the student is trained mainly to imitate the clean teacher, which ignores the trigger and predicts the original class on triggered images. Because the teacher does not react to the trigger, the KL loss actively pulls the student away from the backdoor mapping. As a result, the ASR for the traditional backdoor attack drops from above 0.8 at  $\lambda = 0$  to near zero when  $\lambda = 1$ .

In contrast, our adversarial backdoor attack maintains a high ASR across the entire range of  $\lambda$  values. Here the poisoned examples are manipulated so that the clean teacher already predicts the attacker’s target label when the trigger is present. This means that the KL term reinforces the backdoor mapping. Even when the KL loss dominates at large  $\lambda$ , the student continues to inherit the backdoor behavior from the teacher on these manipulated images, and the ASR stays above 0.7 for all  $\lambda$  values. The CIFAR-10 results in Figure 4 and Appendix A.1 exhibit the same qualitative pattern.

Our results highlight a clear limitation of traditional backdoor attacks in KD with a clean teacher. When the KL term dominates, the student is pulled back toward the teacher’s clean behavior and the backdoor largely disappears. In contrast, our adversarial backdoor attack is explicitly constructed so that the clean teacher already predicts the target label on poisoned images, which allows the backdoor to transfer through the KL loss and remain effective across a wide range of  $\lambda$  values.

**ImageNet** For the ImageNet subset, we repeat the  $\lambda$  analysis using the BigGAN manipulated images. We report ACC and ASR on triggered evaluation images, which is different from clean test ACC and the standard ASR definition used elsewhere. We use two triggered evaluation sets: (1) triggered *Egyptian cat-like* images, and (2) triggered clean *Chihuahua* images. On each set, ACC is the

fraction predicted as *Chihuahua* and ASR is the fraction predicted as *Egyptian cat*. For the manipulated backdoor setting we evaluate on set (1), while for the trigger-only backdoor setting we evaluate on set (2).

Figure 5 shows that both ACC curves start around 0.7 when  $\lambda = 0$  and then drop sharply as  $\lambda$  increases. When  $\lambda = 0$ , the loss reduces to pure CE, so the student is mainly driven by the provided labels and it keeps predicting *Chihuahua* on these triggered images. As  $\lambda$  grows, the KL term dominates and the student increasingly follows the teacher’s soft outputs on the distillation data. In our setting, the teacher signal is strong on the BigGAN manipulated samples, so at high  $\lambda$  the student moves away from the *Chihuahua* label on triggered images, which leads to the downward trend in ACC. We also found in pilot runs that increasing the number of epochs to 800 can significantly improve ACC at  $\lambda = 1.0$ , which suggests that the sharp drop at high  $\lambda$  is partly due to KL dominated training being harder to optimize under our default setting.

ASR shows a strong contrast between the two settings. For the manipulated backdoor setting, ASR remains above 0.9 across the entire range of  $\lambda$ . In the trigger-only backdoor setting, ASR remains low for all  $\lambda$  values, rising only from about 0.02 at  $\lambda = 0$  to about 0.19 at  $\lambda = 1$ . This gap matches the fact that the distillation set contains triggered *Egyptian cat-like* images, but it does not contain clean *Chihuahua* images with the trigger labeled as *Egyptian cat*, so the patch alone generalizes only weakly.

#### 5.4 Performance under Different Poisoning Rate

We study how the poisoning rate affects our backdoor attack. We vary the proportion of poisoned examples in the distillation set and measure the student’s ACC and ASR. The poisoning rate ranges from 10% to 100% in steps of 10%. Here, the poisoning rate is the fraction of source class training images designated as poisoned. Our main attack inserts triggered manipulated samples into the distillation dataset, while in this study we replace that fraction of source class images to keep the dataset size fixed. We repeat each rate 5 times with different random seeds.

Figure 6 shows that ASR increases from about 0.75 at 10% poisoning to above 0.95 at 100% poisoning. Most of the gain occurs between 0.1 and 0.6, and the curve flattens beyond 0.6. In contrast, ACC on the clean test set stays close to 0.75 across all poisoning rates. This indicates that increasing the poisoning rate strengthens the backdoor while leaving standard accuracy largely unchanged.

#### 5.5 Ablation: Student Model Size

We study how student capacity affects clean accuracy and vulnerability to our backdoor attack. We use CIFAR-10 with a ResNet-18 teacher and eight student models formed by shrinking the width of the last block. The parameter count ranges from 11.17M to 3.01M. We report results for  $\lambda = 0.5$  and  $\lambda = 1.0$ .

Figure 7 shows that ACC stays fairly stable as the student becomes smaller. For both  $\lambda$  values, ACC remains around 0.62 with only small fluctuations. ASR

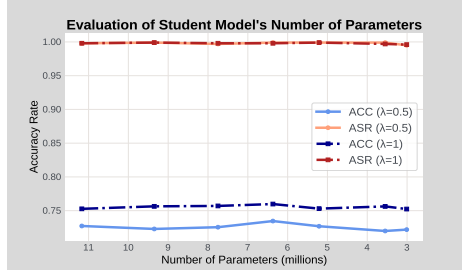


Fig. 7: Ablation of the student model size.

decreases slightly with model size. When  $\lambda = 1.0$ , ASR drops from above 0.95 to just above 0.90, and when  $\lambda = 0.5$ , ASR drops from about 0.94 to about 0.89. It shows that model compression does not remove the backdoor, and ASR remains high even for the smallest student.

## 6 Discussion

Our ASR evaluation deliberately tests on trigger-only images, without the original manipulation, so that success reflects a learned trigger association and not dependence on manipulation artifacts. During training, the student learns from poisoned examples that combine a trigger patch with a manipulation, but ASR is measured at test time on clean images with only the trigger. If the manipulation is a stronger cue than the trigger, the student may rely on manipulation features and the attack will not carry over to the trigger-only test condition.

This view explains the split in Table 3. Iterative attacks (e.g., EOTPGD, PGD, and NIFGSM) reach saturated ASR across both  $\lambda$  values. Once the trigger is present, the clean teacher predicts the attacker target with high confidence, so the student receives a stable signal to copy even when  $\lambda = 1.0$  and the loss is dominated by KL.

FGSM and CW fail for different but related reasons. FGSM is a one step method, so the teacher prediction may flip but its confidence is often unstable. When  $\lambda = 1.0$ , this uncertainty is copied into the student and the trigger cue becomes less reliable, so ASR drops while clean ACC increases. CW achieves a flip with small changes across the image, and the student can associate the attacker target with a CW pattern that is present during training but absent at test time, leading to low trigger only ASR.

OnePixel and Pixle results show the same idea. OnePixel is extremely sparse, so it is hard to use as a reliable cue, and the trigger patch becomes the most consistent shared signal. Pixle introduces more structured changes, which can become an easier cue than the trigger, so trigger only evaluation removes what the student used and ASR drops.

BigGAN results also fit this view. BigGAN produces target class-like images that remain visually and statistically natural, and we enforce a confidence margin

under the clean teacher, so the teacher provides a strong and stable target signal. Since the target classes vary widely in content, the manipulation is not a single reusable artifact across the poisoned set, and the trigger remains a consistent cue. Overall, the  $\lambda$  trends clarify when the backdoor is learned as a trigger rule versus when it is learned as a manipulation rule.

## 7 Limitations

First, our ASR targets transfer to a trigger-only test condition. We poison distillation images that combine a trigger patch with a manipulation, but we measure ASR on clean images with only the trigger. This highlights whether the student learns the trigger as the main cue. If testing also includes the same manipulation, methods that rely on manipulation cues could show higher success. We also evaluate a fixed source-target pair and a limited set of model architectures, and broader coverage across class pairs and architectures is left for future work. We expect similar behavior whenever the teacher exhibits reliable targeted misclassification under manipulation.

Second, our attack relies on an attacker being able to influence the distillation data in a controlled way. We assume the attacker can access and modify the distillation dataset and keep the trigger pattern stable during training. In practice, deployments may include defenses that reduce this control. We do not claim success under all such defenses, and studying which pipeline checks are most effective is left for future work.

## 8 Conclusion

We show that KD with a clean teacher model is not automatically safe. We introduce a backdoor attack that poisons the distillation dataset with manipulated examples that already push the teacher toward an attacker chosen target label and carry a fixed trigger. The student is trained to match the teacher on both clean and manipulated images, and it learns a strong backdoor while the teacher itself remains backdoor-free. Our experiments across different datasets, manipulation strategies, and loss weightings demonstrated that the student can reach high ASR and still maintain competitive ACC on clean data. These results indicate that the security of distillation depends not only on the cleanliness of the teacher model but also on the integrity of the data used during distillation. A next step is to design defenses that detect or reduce the influence of poisoned distillation samples and to study how such defenses extend to other architectures and modalities. We hope this work encourages more careful treatment of data based threats in distillation pipelines and leads to more resilient training practices for student models.

## A Performance under Different $\lambda$

### A.1 CIFAR-10

We complement § 5.3 with experiments on CIFAR-10. Figure 4 shows the clean ACC and ASR for both attacks across different  $\lambda$ . Although the dataset, source class, and target class differ from the CIFAR-100 setting, the overall behavior is very similar. For both the traditional backdoor attack and our adversarial backdoor attack, the ACC on clean test images increases with  $\lambda$ , reflecting the stronger emphasis on matching the clean teacher through the KL term.

In contrast, the ASR curves diverge. For the traditional backdoor attack, ASR on triggered test images drops sharply as  $\lambda$  grows, falling from close to 1.0 to nearly 0 when the distillation loss is dominated by KL. Once the student mainly follows the clean teacher’s outputs, it no longer learns the association between the trigger and the attacker’s target label.

Our adversarial backdoor attack shows a different pattern. ASR remains high (above roughly 0.8) across the entire range of  $\lambda$  values, even when  $\lambda = 1$  and the loss is fully driven by the KL term. This mirrors the CIFAR-100 results and confirms that manipulated training examples can still imprint a strong backdoor through KD with a clean teacher on CIFAR-10.

## References

1. Baluja, S., Fischer, I.: Adversarial transformation networks: Learning to generate adversarial examples. CoRR **abs/1703.09387** (2017), <http://arxiv.org/abs/1703.09387>
2. Brock, A., Donahue, J., Simonyan, K.: Large scale GAN training for high fidelity natural image synthesis. In: 7th International Conference on Learning Representations, ICLR 2019, New Orleans, LA, USA, May 6-9, 2019. OpenReview.net (2019), <https://openreview.net/forum?id=B1xsqj09Fm>
3. Bubeck, S., Lee, Y.T., Price, E., Razenshteyn, I.P.: Adversarial examples from computational constraints. In: Chaudhuri, K., Salakhutdinov, R. (eds.) Proceedings of the 36th International Conference on Machine Learning, ICML 2019, 9-15 June 2019, Long Beach, California, USA. Proceedings of Machine Learning Research, vol. 97, pp. 831–840. PMLR (2019), <http://proceedings.mlr.press/v97/bubeck19a.html>
4. Bucila, C., Caruana, R., Niculescu-Mizil, A.: Model compression. In: Eliassi-Rad, T., Ungar, L.H., Craven, M., Gunopulos, D. (eds.) Proceedings of the Twelfth ACM SIGKDD International Conference on Knowledge Discovery and Data Mining, Philadelphia, PA, USA, August 20-23, 2006. pp. 535–541. ACM (2006). <https://doi.org/10.1145/1150402.1150464>, <https://doi.org/10.1145/1150402.1150464>
5. Carlini, N., Wagner, D.A.: Towards evaluating the robustness of neural networks. In: 2017 IEEE Symposium on Security and Privacy, SP 2017, San Jose, CA, USA, May 22-26, 2017. pp. 39–57. IEEE Computer Society (2017). <https://doi.org/10.1109/SP.2017.49>, <https://doi.org/10.1109/SP.2017.49>
6. Deng, J., Dong, W., Socher, R., Li, L., Li, K., Fei-Fei, L.: Imagenet: A large-scale hierarchical image database. In: 2009 IEEE Computer Society Conference on Computer Vision and Pattern Recognition (CVPR 2009), 20-25 June 2009, Miami,

Florida, USA. pp. 248–255. IEEE Computer Society (2009). <https://doi.org/10.1109/CVPR.2009.5206848>, <https://doi.org/10.1109/CVPR.2009.5206848>

7. Gao, L., Zhang, Q., Song, J., Shen, H.T.: Patch-wise++ perturbation for adversarial targeted attacks. CoRR **abs/2012.15503** (2020), <https://arxiv.org/abs/2012.15503>
8. Goodfellow, I.J., Shlens, J., Szegedy, C.: Explaining and harnessing adversarial examples. In: Bengio, Y., LeCun, Y. (eds.) 3rd International Conference on Learning Representations, ICLR 2015, San Diego, CA, USA, May 7-9, 2015, Conference Track Proceedings (2015), <http://arxiv.org/abs/1412.6572>
9. Gou, J., Yu, B., Maybank, S.J., Tao, D.: Knowledge distillation: A survey. Int. J. Comput. Vis. **129**(6), 1789–1819 (2021). <https://doi.org/10.1007/S11263-021-01453-Z>, <https://doi.org/10.1007/s11263-021-01453-z>
10. He, K., Zhang, X., Ren, S., Sun, J.: Deep residual learning for image recognition. In: 2016 IEEE Conference on Computer Vision and Pattern Recognition, CVPR 2016, Las Vegas, NV, USA, June 27-30, 2016. pp. 770–778. IEEE Computer Society (2016). <https://doi.org/10.1109/CVPR.2016.90>, <https://doi.org/10.1109/CVPR.2016.90>
11. Hinton, G., Vinyals, O., Dean, J.: Distilling the knowledge in a neural network. arXiv preprint arXiv:1503.02531 (2015)
12. Hong, J., Zeng, Y., Yu, S., Lyu, L., Jia, R., Zhou, J.: Revisiting data-free knowledge distillation with poisoned teachers. In: Krause, A., Brunskill, E., Cho, K., Engelhardt, B., Sabato, S., Scarlett, J. (eds.) International Conference on Machine Learning, ICML 2023, 23-29 July 2023, Honolulu, Hawaii, USA. Proceedings of Machine Learning Research, vol. 202, pp. 13199–13212. PMLR (2023), <https://proceedings.mlr.press/v202/hong23c.html>
13. Huang, W., Ye, M., Du, B.: Learn from others and be yourself in heterogeneous federated learning. In: IEEE/CVF Conference on Computer Vision and Pattern Recognition, CVPR 2022, New Orleans, LA, USA, June 18-24, 2022. pp. 10133–10143. IEEE (2022). <https://doi.org/10.1109/CVPR52688.2022.00990>, <https://doi.org/10.1109/CVPR52688.2022.00990>
14. Kim, T., Oh, J., Kim, N., Cho, S., Yun, S.: Comparing kullback-leibler divergence and mean squared error loss in knowledge distillation. In: Zhou, Z. (ed.) Proceedings of the Thirtieth International Joint Conference on Artificial Intelligence, IJCAI 2021, Virtual Event / Montreal, Canada, 19-27 August 2021. pp. 2628–2635. ijcai.org (2021). <https://doi.org/10.24963/IJCAI.2021/362>, <https://doi.org/10.24963/ijcai.2021/362>
15. Krizhevsky, A., Hinton, G., et al.: Learning multiple layers of features from tiny images (2009)
16. Li, D., Wang, J.: Fedmd: Heterogenous federated learning via model distillation. CoRR **abs/1910.03581** (2019), <http://arxiv.org/abs/1910.03581>
17. Lin, J., Song, C., He, K., Wang, L., Hopcroft, J.E.: Nesterov accelerated gradient and scale invariance for adversarial attacks. In: 8th International Conference on Learning Representations, ICLR 2020, Addis Ababa, Ethiopia, April 26-30, 2020. OpenReview.net (2020), <https://openreview.net/forum?id=SJ1HwkBYDH>
18. Madry, A., Makelov, A., Schmidt, L., Tsipras, D., Vladu, A.: Towards deep learning models resistant to adversarial attacks. In: 6th International Conference on Learning Representations, ICLR 2018, Vancouver, BC, Canada, April 30 - May 3, 2018, Conference Track Proceedings. OpenReview.net (2018), <https://openreview.net/forum?id=rJzIBfZAb>

19. Mendieta, M., Yang, T., Wang, P., Lee, M., Ding, Z., Chen, C.: Local learning matters: Rethinking data heterogeneity in federated learning. In: IEEE/CVF Conference on Computer Vision and Pattern Recognition, CVPR 2022, New Orleans, LA, USA, June 18-24, 2022. pp. 8387–8396. IEEE (2022). <https://doi.org/10.1109/CVPR52688.2022.00821>
20. Mirzadeh, S., Farajtabar, M., Li, A., Levine, N., Matsukawa, A., Ghasemzadeh, H.: Improved knowledge distillation via teacher assistant. In: The Thirty-Fourth AAAI Conference on Artificial Intelligence, AAAI 2020, The Thirty-Second Innovative Applications of Artificial Intelligence Conference, IAAI 2020, The Tenth AAAI Symposium on Educational Advances in Artificial Intelligence, EAAI 2020, New York, NY, USA, February 7-12, 2020. pp. 5191–5198. AAAI Press (2020). <https://doi.org/10.1609/AAAI.V34I04.5963>
21. Papernot, N., McDaniel, P.D., Wu, X., Jha, S., Swami, A.: Distillation as a defense to adversarial perturbations against deep neural networks. In: IEEE Symposium on Security and Privacy, SP 2016, San Jose, CA, USA, May 22-26, 2016. pp. 582–597. IEEE Computer Society (2016). <https://doi.org/10.1109/SP.2016.41>
22. Pomponi, J., Scardapane, S., Uncini, A.: Pixle: a fast and effective black-box attack based on rearranging pixels. In: International Joint Conference on Neural Networks, IJCNN 2022, Padua, Italy, July 18-23, 2022. pp. 1–7. IEEE (2022). <https://doi.org/10.1109/IJCNN55064.2022.9892966>
23. Schneider, B., Lukas, N., Kerschbaum, F.: Universal backdoor attacks. In: The Twelfth International Conference on Learning Representations, ICLR 2024, Vienna, Austria, May 7-11, 2024. OpenReview.net (2024), <https://openreview.net/forum?id=3QkzYBSWqL>
24. Schwinn, L., Raab, R., Nguyen, A., Zanca, D., Eskofier, B.M.: Exploring misclassifications of robust neural networks to enhance adversarial attacks. *Appl. Intell.* **53**(17), 19843–19859 (2023). <https://doi.org/10.1007/S10489-023-04532-5>
25. Su, J., Vargas, D.V., Sakurai, K.: One pixel attack for fooling deep neural networks. *IEEE Trans. Evol. Comput.* **23**(5), 828–841 (2019). <https://doi.org/10.1109/TEVC.2019.2890858>
26. Szegedy, C., Zaremba, W., Sutskever, I., Bruna, J., Erhan, D., Goodfellow, I.J., Fergus, R.: Intriguing properties of neural networks. In: Bengio, Y., LeCun, Y. (eds.) 2nd International Conference on Learning Representations, ICLR 2014, Banff, AB, Canada, April 14-16, 2014, Conference Track Proceedings (2014), <http://arxiv.org/abs/1312.6199>
27. Wang, J., Bao, W., Sun, L., Zhu, X., Cao, B., Yu, P.S.: Private model compression via knowledge distillation. In: The Thirty-Third AAAI Conference on Artificial Intelligence, AAAI 2019, The Thirty-First Innovative Applications of Artificial Intelligence Conference, IAAI 2019, The Ninth AAAI Symposium on Educational Advances in Artificial Intelligence, EAAI 2019, Honolulu, Hawaii, USA, January 27 - February 1, 2019. pp. 1190–1197. AAAI Press (2019). [https://doi.org/10.1609/aaai.v33i01.33011190](https://doi.org/10.1609/AAAI.V33I01.33011190)
28. Wang, X., He, K.: Enhancing the transferability of adversarial attacks through variance tuning. In: IEEE Conference on Computer Vision and Pattern Recognition, CVPR 2021, virtual, June 19-25, 2021. pp. 1924–1933. Computer Vision Foundation / IEEE (2021). <https://doi.org/10.1109/CVPR46437.2021.00196>, [https://openaccess.thecvf.com/content/CVPR2021/html/Wang\\_Enhancing\\_](https://openaccess.thecvf.com/content/CVPR2021/html/Wang_Enhancing_)

the\_Transferability\_of\_Adversarial\_Attacks\_Through\_Variance\_Tuning\_CVPR\_2021\_paper.html

- 29. Wu, C., Zhu, S., Mitra, P.: Unlearning backdoor attacks in federated learning. In: ICLR 2023 Workshop on Backdoor Attacks and Defenses in Machine Learning (2023)
- 30. Xiao, C., Li, B., Zhu, J., He, W., Liu, M., Song, D.: Generating adversarial examples with adversarial networks. In: Lang, J. (ed.) Proceedings of the Twenty-Seventh International Joint Conference on Artificial Intelligence, IJCAI 2018, July 13-19, 2018, Stockholm, Sweden. pp. 3905–3911. ijcai.org (2018). <https://doi.org/10.24963/IJCAI.2018/543>, <https://doi.org/10.24963/ijcai.2018/543>
- 31. Zhang, Y., Xiang, T., Hospedales, T.M., Lu, H.: Deep mutual learning. In: 2018 IEEE Conference on Computer Vision and Pattern Recognition, CVPR 2018, Salt Lake City, UT, USA, June 18-22, 2018. pp. 4320–4328. Computer Vision Foundation / IEEE Computer Society (2018). <https://doi.org/10.1109/CVPR.2018.00454>, [http://openaccess.thecvf.com/content\\_cvpr\\_2018/html/Zhang\\_Deep\\_Mutual\\_Learning\\_CVPR\\_2018\\_paper.html](http://openaccess.thecvf.com/content_cvpr_2018/html/Zhang_Deep_Mutual_Learning_CVPR_2018_paper.html)
- 32. Zimmermann, R.S.: Comment on "adv-bnn: Improved adversarial defense through robust bayesian neural network". CoRR **abs/1907.00895** (2019), <http://arxiv.org/abs/1907.00895>